Progress in Earth and Planetary Science

RESEARCH ARTICLE Open Access

Widespread distribution of radiocesium-bearing microparticles over the greater Kanto Region resulting from the Fukushima nuclear accident

Yoshinari Abe[1,2*], Seika Onozaki[1], Izumi Nakai[1], Kouji Adachi[3], Yasuhito Igarashi[4,5], Yasuji Oura[6], Mitsuru Ebihara[6,7], Takafumi Miyasaka[3,8,9], Hisashi Nakamura[8], Keisuke Sueki[10], Haruo Tsuruta[11] and Yuichi Moriguchi[12]

Abstract

The Fukushima Daiichi Nuclear Power Plant (FDNPP) accident in March 2011 emitted a considerable amount of radioactive materials. This study isolated radiocesium-bearing microparticles (CsMPs), a form of radioactive materials emitted from the FDNPP at the early stage of the accident, from aerosols collected hourly on filter tapes at seven monitoring stations at the greater Kanto Region, including the Tokyo metropolitan area, on 15 March 2011. The aerosols had a spherical shape ~ 1 μm in diameter with activity of less than 1 Bq of ^{137}Cs per particle. Their physical and chemical characteristics, including radioactivity ratio ^{134}Cs/^{137}Cs as well as chemical composition and state, are essentially the same as previously reported CsMPs. This study demonstrated that air parcels containing CsMPs emitted from the FDNPP were widespread over the greater Kanto Region, more than 250 km away from the FDNPP, during the daytime of 15 March. Trajectory analysis indicated that these particles were emitted from the reactor No. 2 of FDNPP between 14 March evening and 15 March early morning. The information obtained on the widespread distribution of CsMPs can be useful for assessing the actual impacts of radioactive contamination from the FDNPP accident on the environment and human health.

Keywords: Fukushima Daiichi Nuclear Power Plant accident, Radiocesium-bearing microparticle, Suspended particulate matter, Synchrotron radiation X-ray analysis, Trajectory analysis

1 Introduction

Considerable amounts of radioactive materials were released into the environment following the Fukushima Daiichi Nuclear Power Plant (FDNPP) accident caused by tsunamis associated with the Tohoku Earthquake on 11 March 2011 (e.g., MEXT 2020; Steinhauser et al. 2014). To reveal the time evolution of atmospheric radionuclide concentrations immediately after the accident, Tsuruta et al. (2014, 2018) and Oura et al. (2015) investigated suspended particulate matter (SPM) collected on filter-tape at automated air pollution monitoring stations across Eastern Japan. More than 400 stations in Eastern Japan were in operation during the initial period of the FDNPP accident. Analyzing atmospheric radiocesium concentrations at 99 of those SPM monitoring stations, these studies revealed that radioactive materials emitted into the air from the FDNPP were transported over Eastern Japan via several major plumes during 12–23 March (Tsuruta et al. 2014, 2018).

* Correspondence: y.abe@mail.dendai.ac.jp
[1]Department of Applied Chemistry, Faculty of Science, Tokyo University of Science, 1-3 Kagurazaka, Shinjuku-ku, Tokyo 162-8601, Japan
[2]Division of Material Science and Engineering, Graduate School of Engineering, Tokyo Denki University, 5 Senju Asahi-cho, Adachi-ku, Tokyo 120-8551, Japan
Full list of author information is available at the end of the article

As a form of radioactive materials emitted from the FDNPP at the early stage of the accident, radiocesium-bearing microparticles (CsMPs) have been investigated by numerous researchers in recent years (Igarashi et al. 2019). They were solid particles and not easily dissolved into water, which first discovered by Adachi et al. (2013) from aerosols collected at the Meteorological Research Institute (MRI) in Tsukuba, 170 km south-southwest of FDNPP, during 2110 JST 14 March and 0910 JST 15 March 2011. After the discovery of the CsMP, many studies focused on their physical and chemical characteristics as well as their environmental distributions (Igarashi et al. 2019). While several types of CsMPs have been reported, almost CsMPs examined previously were nearly spherical, several μm in diameter, and had relatively high specific radioactivity, i.e., ~ 1 Bq per particle as ^{137}Cs (Adachi et al. 2013; Furuki et al. 2017). Their main matrices were silicate glass (Satou et al. 2016) with Fe and Zn (Adachi et al. 2013; Abe et al. 2014), and trace amounts of various heavy elements associated with nuclear fuel and fission products (FPs) were detected (Abe et al. 2014). Physical and chemical characterizations of radioactive materials, including their water solubility, shape, size, and chemical composition and state, are critical factors that determine their behavior within the environment and human body. CsMPs and other particulate radioactive materials have previously been identified in various environmental samples collected in Fukushima Prefecture as follows: soils collected around the FDNPP (e.g., Satou et al. 2016, 2018, Ono et al. 2017, Furuki et al. 2017, Martin et al. 2019, 2020), a non-woven fabric cloth laid on an agricultural field (Yamaguchi et al. 2016), and river sediments (Miura et al. 2018). Similar radioactive microparticles were also found on masks worn during cleaning work in residential areas near the FDNPP 5 years after the accident (Higaki et al. 2017). As mentioned above, these CsMPs found previously consist primarily of silicate glass. It is thus concerned that they have a long-term impact on the environment compared to water-soluble radioactive materials, whereas some recent investigations indicate a very slow rate of dissolution of CsMP into pure-water or seawater (Okumura et al. 2019; Suetake et al. 2019). Meanwhile, some CsMPs containing chloride as a water-soluble compound had been recently found from aerosols collected near the FDNPP after the hydrogen explosion of the reactor No. 1 of the FDNPP (Onozaki et al. 2019). Comprehensive investigations of CsMPs with various physical/chemical properties are therefore vitally important in accurately assessing the impacts of radioactive contamination from the FDNPP accident on the environment and human health.

Among the major polluted plumes identified by Tsuruta et al. (2014), the second plume (P2) carried the aerosols collected at the MRI on 14 and 15 March 2011 (Adachi et al. 2013). After being observed at SPM monitoring stations in the vicinity of the MRI (Tsukuba) during the morning of 15 March, P2 was then spread into the Kanto Plain, including the Tokyo metropolitan area, one of the most populated areas in the world. The southward spread of P2 was due to low-level northerlies associated with an eastward-moving low-pressure system located south of the Kanto Region (Takemura et al. 2011). Hypothesizing that CsMPs were the major carrier of radioactive Cs in P2, this study aims to verify the widespread distribution of CsMP in P2 over the greater Kanto Region (in and around the Kanto Region) on 15 March, focusing on how far CsMPs were transported southwest from the FDNPP by the local wind system. We examined radioactive aerosol particles from the SPM filter-tape samples collected hourly on 15 March at several stations in the greater Kanto Region to compare their physical/chemical characteristics with those of previously reported CsMPs isolated from various environmental samples. To investigate detailed chemical characteristics of the radioactive aerosols isolated from the SPM filter-tape samples, we applied multiple X-ray analytical techniques using a synchrotron radiation microbeam (SR-μ) X-ray in a nondestructive manner. The SR-μ-X-ray analysis is an analytical technique that is commonly used for microscopic chemical characterization of various materials in the nondestructive manner and is quite suitable for CsMPs as demonstrated by several previous studies (Abe et al. 2014; Ono et al. 2017; Onozaki et al. 2019; Miura et al. 2020; Kurihara et al. 2020a). This study has implications for the impacts of radioactive materials on the environment and human health as well as the reactor condition during the early stage of the accident.

2 Methods/experimental

2.1 SPM filter-tape samples and separation method of particles

The SPM monitors within the Japan air pollution monitoring network are routinely operated by local governments (prefectures and municipalities designated by ordinance). Particulates less than 10 μm in diameter were automatically collected on the filter tape installed in the SPM monitors as a sample spot (11 or 16 mm in diameter) for 1 h at a flow rate of 15.0, 16.7, or 18.0 l/min. The filter tape was made of glass fiber or polytetrafluoroethylene. Detailed information of the SPM filter-tape samples has been described in previous studies (Tsuruta et al. 2014, 2018; Oura et al. 2015). Seven pieces of the filters sampled at seven monitoring stations designated as A, B, C, D, E, F, and G within the greater Kanto Region (see Table 1 and Fig. 1) were used in this study. Each piece was selected which had the highest

Table 1 Information of seven monitoring stations (A~G) and SPM filter-tape samples investigated in the present study

Station	Latitude	Longitude	Distance from FDNPP	Sampling time (JST)	^{137}Cs/Bq m^{-3}
A	35.85	140.25	189 km	15 March 0800–0900	22.1
B	36.19	139.13	218 km	15 March 1200–1300	59.1
C	35.78	139.62	229 km	15 March 1000–1100	81.9
D	35.65	139.59	236 km	15 March 1000–1100	29.4
E	35.37	139.22	280 km	15 March 1400–1500	29.3
F	36.33	138.44	261 km	15 March 1600–1700	22.1
G	36.41	138.24	273 km	15 March 1600–1700	32.8

^{137}Cs concentration on March 15 at each station under the direct influence of P2. We cut these filters into four or eight portions in collecting radioactive particles. An imaging plate (GE Measurement and Control, CR × 25P computed radiography scanner) and micromanipulator (AP-xy-01; Micro Support Corp.) were used to detect and separate radioactive particles from the filters. The amount and distribution of radioactive particles on the filter was observed in a process similar to previous studies (Adachi et al. 2013; Abe et al. 2014). Prior to the SR experiments, a low-vacuum scanning electron microscope (SEM; SU 3500; Hitachi High-Technologies) was used to observe the shapes of individual particles isolated from the filters. The radioactivity of ^{134}Cs and ^{137}Cs in each particle was determined by using a Ge semiconductor detector (GC4018; CANBERRA) coupled with a multichannel analyzer (Lynx Digital Signal Analyzer; CANBERRA). The gamma-ray spectrum was collected for more than 400,000 s per particle. Two standard radioactive sources, ^{134}Cs standard by Japan Radioisotope Association and ^{137}Cs standard by Amersham plc, were measured in the same manner to

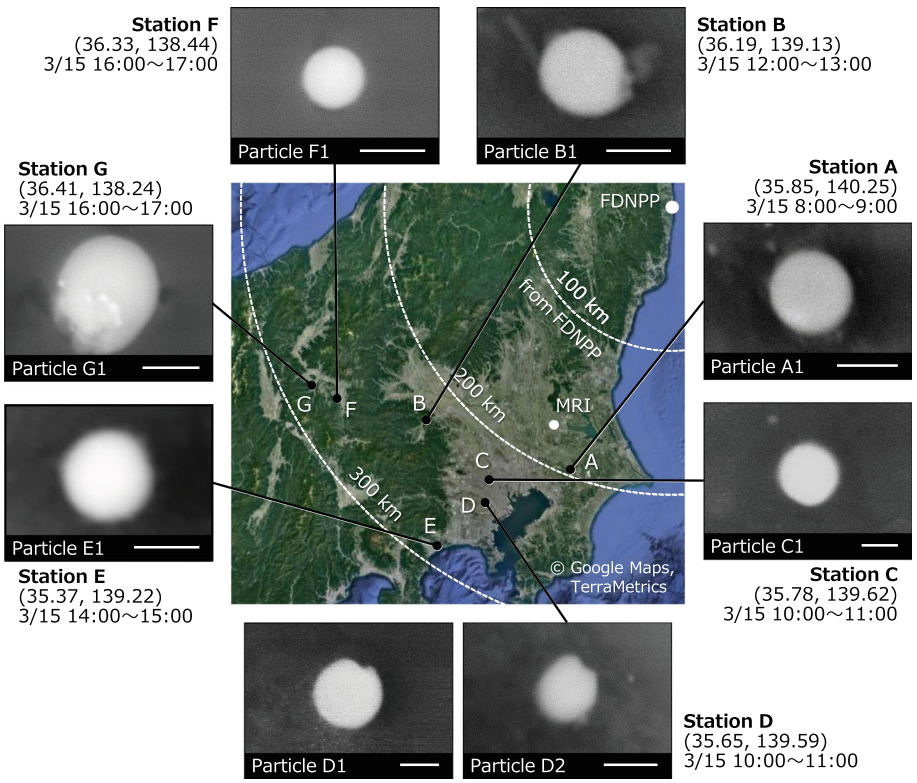

Fig. 1 Locations of monitoring stations A~G in the greater Kanto Region and radioactive particles isolated in this study. Coordinates and collection time of the filters are shown for each station. White dashed lines on the map indicate distance from the FDNPP. Eight CsMPs were isolated from these seven filters as displayed by SEM images around the map. They are nearly spherical in shape with a diameter of 1.3 μm (particle A1), 1.3 μm (B1), 1.4 μm (C1), 1.5 μm (D1), 1.2 μm (D2), 1.3 μm (E1), 0.9 μm (F1), and 1.8 μm (G1). The scale bars under the SEM images show a length of 1 μm

calibrate radioactivity of the particles. Absolute value and statistical error of radioactivity of ^{134}Cs and ^{137}Cs in individual particles were calculated as decay-corrected data at the time of 1446 JST 11 March 2011. After these analyses, the radioactive particles on carbon tape fragments were removed and then placed on a flat Kapton tape with a plastic holder for the SR-μ-X-ray analyses.

2.2 Synchrotron radiation X-ray analyses of CsMPs

The SR experiments using an X-ray microbeam were carried out at the BL37XU (Terada et al. 2004, 2010), a hard X-ray undulator beamline at SPring-8, located at the Japan Synchrotron Radiation Research Institute (JASRI). The sample was placed on an automatic XY stage in the experimental hatch. Monochromatic X-rays were obtained with a Si (111) double crystal monochromator, and the X-ray microbeam with the size of ~ 1 μm (V) × ~1 μm (H) was produced by focusing Kirkpatrick–Baez mirrors. We applied three X-ray analytical techniques: SR-μ-X-ray fluorescence (XRF) analysis, SR-μ-X-ray absorption near edge structure (XANES) analysis, and SR-μ-X-ray powder diffraction (XRD) analysis. The measurement conditions of the SR-experiments were the same as in our previous investigations (Abe et al. 2014; Ono et al. 2017; Onozaki et al. 2019).

The SR-μ-XRF analysis was carried out using 37.5 keV X-rays that enable to excite K-edges of Cs (36.0 keV) and Ba (37.4 keV). Three types of energy-dispersive X-ray detectors were used depending on the beamtime: a Si (Li) detector for the beamtimes until 2017, and eight-elements silicon drift detectors or a Ge semiconductor detector for the beamtimes in 2018 and 2019. The SR-μ-XRF spectrum was measured for 200 s in live time per sample. The intensity of each spectrum was normalized to that of the Thomson scattering peak detected at 37.5 keV. The SR-μ-XANES spectra of the particles and the reference samples were measured in fluorescence mode for the following absorption edges: Fe-K edge (7111 eV), Zn-K edge (9661 eV), Mo-K edge (20,000 eV), and Sn-K edge (29,200 eV). The intensity of Kα line of each target elements in individual particles was scanned with a measurement step of ~ 1 eV/step, integration times of 3.0~10.0 s/step, and an energy range of ~ 100 eV from the lower to the higher energy sides of the absorption edge. To normalize the Kα intensity of the target elements, an intensity of the incident X-ray beam (I_0) was monitored using an ionization chamber. Reference materials (powders of metals, typical oxides, sulfides, silicates, and synthesized glass samples) containing each target elements were also measured as a same manner. In the SR-μ-XRD analysis, the X-ray diffraction patterns of the samples were measured with a Debye–Scherrer optical system using a two-dimensional detector (CMOS flat panel) placed 200 mm behind the sample. The energy of the incident X-ray was set to 15.0 keV with an exposure time of 440 ms and an integration of 100 times/sample.

2.3 Trajectory analysis for the radioactive plume transport

A meteorological trajectory analysis was conducted to evaluate air parcel positions every 10 min based on wind fields from the Japan Meteorological Agency mesoscale-model objective analysis. The analysis has a horizontal resolution of 0.0625 × 0.05° with 50 vertical levels up to 21,800 m. Three-hourly analysis data of wind on model levels were used, as well as 3-hourly analysis and 1-hourly forecast data of 10 m surface wind. The three-dimensional wind data cannot resolve small-scale turbulence that is most vigorous within the mixed layer. Air parcels were initially placed at 50 m intervals from 50 m to 1000 m above the surface. For each parcel, the trajectory calculation was terminated if it hit the surface.

3 Results and discussion

3.1 Physical/chemical characteristics of CsMPs isolated from SPM filter-tape

In total, eight CsMPs were successfully isolated from seven pieces of SPM filter-tape samples. As illustrated in Fig. 1, the eight CsMPs were labelled as A1, B1, C1, D1, D2, E1, F1, and G1 in corresponding to the seven SPM monitoring stations. The particles were spherical with diameters of ~ 1 μm, and their radioactivity was less than 1 Bq of ^{137}Cs per particle (Fig. 2). The radioactivity ratios between ^{134}Cs and ^{137}Cs (^{134}Cs/^{137}Cs) were ~ 1.0, suggesting that these particles were emitted from either reactor No. 2 or 3 of FDNPP (Nishihara et al. 2010) (see additional data Table S1 online). As first pointed out by Satou et al. (2018), CsMPs from the FDNPP can be categorized into two major types, type A and type B, based on the ^{134}Cs/^{137}Cs ratio of individual particles. Type A particles are characterized by ^{134}Cs/^{137}Cs ratio of ~ 1.0, in contrast to type B particles with ^{134}Cs/^{137}Cs ratio of ~ 0.9.

As a result of the SR-μ-XRF analyses of individual particles, A1~G1 were found to have qualitatively-similar chemical compositions. The SR-μ-XRF spectra of four representative particles (A1, B1, C1, and E1) are shown in Fig. 3 with that of a type A CsMP collected at the MRI in a previous study (Abe et al. 2014). Note that all these spectra were measured using the same Si (Li) detector in several beamtimes. The XRF analysis using a monochromatic SR-μ-X-ray with high-energy (37.5 keV) for the excitation can detect trace amounts of heavy elements within individual particles, although lighter elements (such as Si) that are major components of the particle could not be detected in the spectrum. In addition to sharp K-line peaks of Cs which had been identified by the gamma-ray spectroscopy, the following eight heavy elements were detected in all particles: Fe,

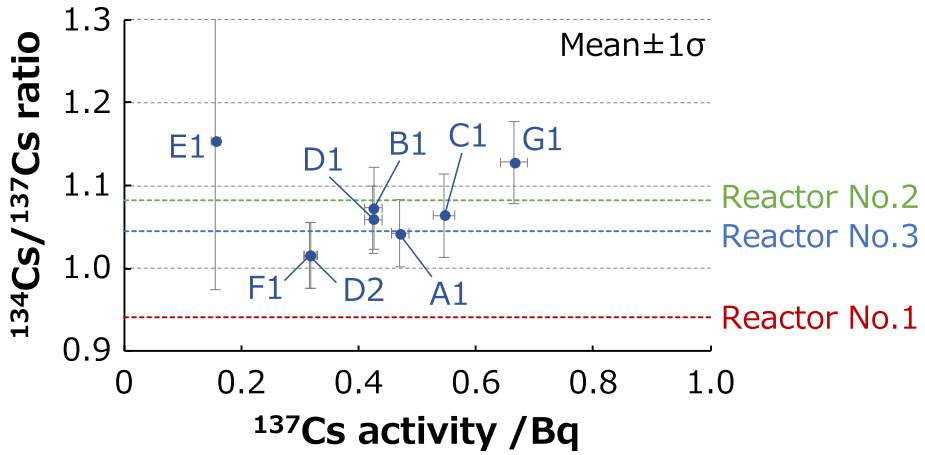

Fig. 2 Radioactivity of ^{137}Cs and ^{134}Cs/^{137}Cs activity ratio of individual particles. The radioactivity of ^{137}Cs (± 1 × standard deviation, σ) of eight particles (A1~G1) are as follows: 0.471 ± 0.016 Bq (particle A1), 0.426 ± 0.015 Bq (B1), 0.546 ± 0.019 Bq (C1), 0.425 ± 0.014 Bq (D1), 0.318 ± 0.011 Bq (D2), 0.156 ± 0.008 Bq (E1), 0.317 ± 0.011 Bq (F1), and 0.665 ± 0.023 Bq (G1). The three dashed lines show estimates of the ^{134}Cs/^{137}Cs ratio of nuclear fuel in FDNPP reactors No. 1, 2, and 3, respectively, at the time of the accident, as calculated using ORIGEN2 Code (Nishihara et al. 2010). Activity values shown here were decay-corrected as of 11 March 2011

Zn, Rb, Mo, Sn, Sb, Te, and Ba. Several trace elements specific to certain particles were also found: Zr from seven particles except for particle B1; Nb from particle C1; Ag from particle F1, Cd from particles C1 and G1; Pb from particles A1, B1, C1, E1, F1, and G1; and U from particles A1, B1, and F1.

The SR-μ-XANES analysis examined the chemical states of four metal elements (Fe, Zn, Mo, and Sn) and indicated that these elements exist as cations in silicate glass with high oxidation numbers (see additional data Fig. S1 online). SR-μ-XRD analysis of individual particles showed no diffraction peaks caused by crystal structure for any of the particles (see additional data Fig. S2 online), confirming that these particles have glass bodies.

As discussed above, physical/chemical characteristics obtained for the eight CsMPs (A1~G1) collected at the seven SPM monitoring stations in the greater Kanto Region are essentially the same as those of type A CsMPs found in the previous studies (e.g., Abe et al. 2014; Igarashi et al. 2019). As first reported by Utsunomiya et al. (2019), it is already-known fact that air parcels containing type A CsMPs passed over Tokyo City at some point on 15 March. Our results strongly support their pioneering report. At the same time, this paper first demonstrated that CsMPs emitted from the FDNPP were widespread over the greater Kanto Region, including West side of Tokyo metropolitan area, during the daytime of 15 March with a temporal resolution of an hour.

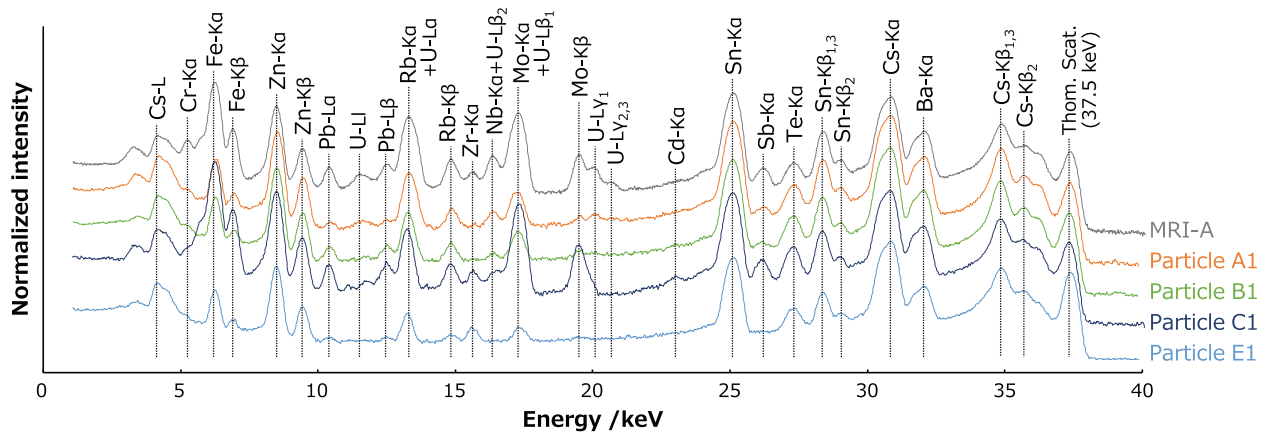

Fig. 3 SR-μ-XRF spectra of four representative CsMPs (A1, B1, C1, and E1) isolated from the SPM filter-tape samples, showing the heavy elemental composition of individual particles. The intensity of each spectrum is displayed on a logarithmic scale and shifted in a longitudinal direction. The spectrum of MRI-A shows datum obtained for one of type A CsMPs (particle A) collected at the MRI in the previous study (Abe et al. 2014)

3.2 Transport pathway of CsMP from FDNPP to greater Kanto Region

To estimate the emission time of the CsMPs and identify their transport pathway(s) from the FDNPP to the greater Kanto Region, we conducted trajectory analysis of air parcels that passed over the seven monitoring stations A~G. As an example, Fig. 4 shows backward trajectories for air parcels situated at different heights over station B starting at 1200 JST 15 March, where the SPM aerosols including particle B1 were collected during 1200–1300 JST. The trajectories are color-coded to distinguish parcel heights at station B in Fig. 4a and also color-coded by parcel height at each time step in Fig. 4b. Figure 4a, b suggests that the air parcels situated at 150–600 m above station B at 1200 JST were likely to be located below the 500 m level within 20 km range from the FDNPP sometime between 0040 and 0330 JST on the same day. The vertical profile of potential temperature at station B (Fig. 4c) indicates that the atmospheric mixed layer was as deep as 800 m above the surface, suggesting that air parcels within the layer should have experienced vigorous turbulent mixing and thus be well-mixed down to near-surface levels. Likewise, air parcels from the FDNPP were released into the night-time mixed layer. Advected by low-level northerlies, these air parcels then travelled along the coast mostly within the marine mixed layer (Fig. 4b), which was probably well developed in the early morning given the cool offshore northerlies over the relatively warm ocean.

Results of our backward trajectory analysis for the seven monitoring stations are summarized in Table 2. Although the estimated emission times have ranges that span several hours, we concluded that polluted air parcels containing CsMPs that passed over the greater Kanto Region on 15 March were emitted from the FDNPP between the evening of 14 March and early morning 15 March. After being released into the mixed layer, these polluted air parcels were advected southward by low-level northerlies and later by northeasterlies. The parcels very likely underwent vigorous mixing down to near-surface levels, within the mixed layer above the stations. The earliest emission time is estimated for the parcels above station E, as the trajectories detoured far offshore under the northwesterlies shortly after emitted. Our trajectory analysis implies that individual aerosol particles that were emitted locally from the FDNPP subsequently spread widely over the greater Kanto Region within a relatively short period of time (within 18 h at the longest) under time-varying flow conditions. Based on the results of our backward trajectory analysis, we calculated forward trajectories for air parcels over the FDNPP starting at 0100 JST 15 March 2011 and showed them on the map with the seven monitoring stations A~G (Fig. 5). The air parcels situated above the FDNPP at that time moved southward and then widespread over the greater Kanto Region within a day.

3.3 Possible source of CsMPs distributed over greater Kanto Region

The chemical composition of particles emitted primarily from the FDNPP could reflect the reactor condition during the early stages of the accident. As indicated by Okumura et al. (2019), we cannot ignore the possibility that CsMP collected from soils years after the accident was altered physically or chemically in the environment even if they are hardly soluble into the water. Unlike such field samples, there would be little change in physical and chemical properties of the CsMPs as they were sampled on the SPM filter-tape shortly after emission. The

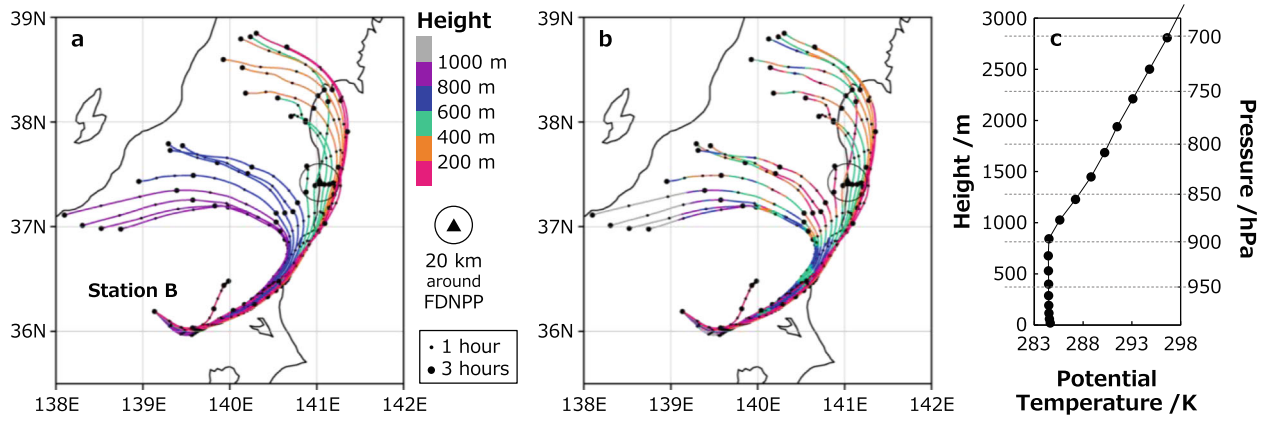

Fig. 4 Backward trajectories calculated for air parcels placed above station B at 1200 JST 15 March 2011. The trajectories are color-coded (**a**) to distinguish heights (m) of the parcels at station B and (**b**) according to their heights at each time step. Small and large dots on the trajectories indicate intervals of every hour and 3 h, respectively, after the calculation start time. **c** Vertical profile of potential temperature (K) above station B at the trajectory start time

Table 2 Summary of the backward trajectory analysis for seven monitoring stations (A~G)

Station	Starting time (JST) of backward trajectories	Depth of atmospheric mixed layer above the station	Estimated paths of air parcels between the station and 20 km range from FDNPP		
			Height above the station	Height above 20 km range from FDNPP	Estimated emission time (JST) from FDNPP
A	15 March 0800	~500 m	750-800 m	0-600 m	15 March 0000-0220
B	15 March 1200	~800 m	150-600 m	0-500 m	15 March 0040-0330
C	15 March 1100	~900 m	800-900 m	100-700 m	15 March 0210-0340
D	15 March 1100	~900 m	850-900 m	50-650 m	15 March 0120-0310
E	15 March 1400	~700 m	750-850 m	100-650 m	14 March 2000- 15 March 0130
F	15 March 1600	~200 m	50-650 m	50-550 m	15 March 0040-0340
G	15 March 1600	~200 m	50-300 m	100-300 m	14 March 2330- 15 March 0200

chemical compositions of the CsMPs discussed in this study are thus likely to be preserved except for radioactive decay effects. Therefore, our analysis offers important information regarding raw materials and the generation process of CsMP in the reactor. All elements identified in the CsMPs can be associated with materials in the FDNPP. As a result of the nuclear fission reaction of ^{235}U, the FPs yielded 11 elements (Rb, Zr, Nb, Mo, Ag, Cd, Sn, Sb, Te, Cs, and Ba) (Crouch 1977, Burns et al. 2012, Yamamoto 2012). It is also possible that Zr and Sn in the CsMPs originate to Zr–Sn alloy used for fuel cladding within the reactors. On the other hand, vaporous elements, such as Rb (e.g., the boiling points of RbOH and RbI are about 1660 K and 1577 K under 1 atm, respectively) and Cs (e.g., the boiling points of CsOH and CsI are about 1263 K and 1553 K under 1 atm, respectively), in the CsMPs were richer than the original composition of FPs derived from U fuel. Therefore, condensation of these elements by vaporization in the reactor pressure vessel (RPV) could happen during the particle generation process. Moreover, the amounts of Cs in the particles would be higher than those of Mo even considering the difference in excitation efficiency from monochromatic X-rays (37.5 keV). Although Cs_2MoO_4 was suggested as one possible source for the vapor phases carrying Cs at high temperature (Kissane and Drosik 2006; Gouello et al. 2013; Do et al. 2018), our result indicates that the volatilization and condensation of Cs_2MoO_4 were not predominant processes of the generating of the CsMPs. Do et al. (2018) have pointed out that CsOH is the predominant cesium species when the damaged fuel temperature is higher than 2000 K at higher steam pressures, but Cs_2MoO_4 would become more important at lower temperature. In this connection, Imoto et al. (2017) reported the presence of nanoparticles of $CsFeSi_2O_6$ within CsMP and pointed out that the material could be formed by the CsOH chemisorption onto Si-bearing stainless steel. Iron, Cr, Mn, Ni, and Mo could originate from stainless steel, which composed RPV and FDNPP buildings. Regarding a possible source for Zn, we previously identified an additive agent of primary cooling water (Abe et al. 2014), but a thin plating of steel and inorganic paint on RPV and buildings could be other potential sources (Itou et al. 2018). Lead metal and Pb-containing materials are commonly used for shielding of radiation. To make a more detailed interpretation of the generation process of the CsMPs, it is indispensable to carry out further scientific investigation using other analytical methods to reveal more quantitative chemical composition and isotopic features of individual particles, such as secondary ion mass spectrometry (Imoto et al. 2017; Kurihara et al. 2020a; Kurihara et al. 2020b).

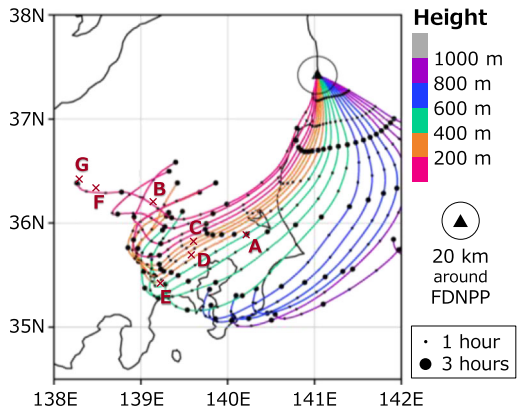

Fig. 5 Forward trajectories calculated for air parcels placed above the FDNPP at 0100 JST 15 March 2011. The trajectories are color-coded to distinguish heights (m) of the parcels at FDNPP. Small and large dots on the trajectories indicate intervals of every hour and 3 h since the calculation start time, respectively

As described above, type A CsMPs including eight particles investigated in this study have been thought to be originated to either reactors No. 2 or No. 3 of the FDNPP based on their $^{134}Cs/^{137}Cs$ ratio: there are two opinions about from which the type A CsMPs were emitted (e.g., Igarashi et al. 2019; Ikehara et al. 2020). We therefore consider the source of the type A CsMPs in relationship to the accident progress, making use of high time-resolution of the SPM filter-tape samples. Our trajectory analysis suggests that the emission time for the

type A CsMPs isolated from the greater Kanto Region was between midnight and early morning 15 March, although emission time could have been as early as the evening of 14 March for parcels that reached station E (Table 2). Consistent with these estimated emission times, pressure inside the RPV in reactor No. 2 decreased after the usage of a safety relief valve around 1903 JST on 14 March, followed by three sharp RPV pressure peaks around 2100 and 2300 JST 14 March and 0100 JST 15 March (TEPCO 2015). Around 0300 JST on 15 March, the pressure inside the primary containment vessel of reactor No. 2 exceeded its designed value (TEPCO 2015). In contrast, no incident was reported for reactor No. 3 during the same period except for a hydrogen explosion at 1101 JST 14 March. We therefore hypothesized that the incident(s) in reactor No. 2 were the most likely cause of the type A CsMPs, rather than reactor No. 3. Our hypothesis is strongly supported by recent investigation of isotopic ratios of U and Cs in CsMPs (Kurihara et al. 2020b).

4 Conclusions

Eight CsMPs were isolated successfully from aerosol particles collected hourly on filter tapes at seven monitoring stations in the greater Kanto Region, including the Tokyo metropolitan area, on 15 March 2011. Our finding demonstrates clearly that air parcels containing CsMPs emitted from the FDNPP were widespread over the greater Kanto Region, farther than 250 km away from the FDNPP, during the daytime of 15 March. Detailed physical and chemical properties of individual CsMPs were investigated by SR-μ-X-ray analyses. As a result, it was concluded that the incident(s) in reactor No. 2 of FDNPP were the most likely cause of CsMPs distributed over the greater Kanto Region. Our trajectory analysis also suggests that air parcels containing the CsMPs as water-insoluble microparticles with radionuclides likely passed over the greater Kanto Region including Tokyo metropolitan area on 15 March. Some of those particles could have been deposited on the ground or suspended in the near-surface air, although most of them were transported to the ocean. Further investigation is necessary to estimate the environmental and health impacts from the CsMPs that travelled into the metropolitan area. Information regarding widespread distribution of CsMPs can be useful toward calculating an inhalation dose of radionuclides during the early stage of the accident.

5 Supplementary Information

The online version contains supplementary material available at https://doi.org/10.1186/s40645-020-00403-6.

Additional file 1: Table S1. ^{134}Cs and ^{137}Cs radioactivities and $^{134}Cs/^{137}Cs$ activity ratio of eight particles (A1~G1). **Figure S1.** SR-μ-XANES spectra of four representative CsMPs (A1, B1, C1, and E1) isolated from the SPM filter and reference materials. (a) Fe-K edge, (b) Zn-K edge, (c) Mo-K edge, and (d) Sn-K edge. **Figure S2.** SR-μ-XRD patterns of four representative radioactive particles (A1, B1, C1, and E1) isolated from the SPM filter and reference material. (a) Particle A1, (b) particle B1, (c) particle C1, (d) particle E1, and (e) silicon powder (NIST SRM 640c). In contrast to sharp diffraction peaks detected in silicon powder, no obvious peaks were detected in four radioactive particles.

Abbreviations

FDNPP: Fukushima Daiichi Nuclear Power Plant; SPM: Suspended particulate matter; CsMP: Radiocesium-bearing microparticle; JST: Japan Standard Time; MRI: Meteorological Research Institute; FP: Fission product; SR-μ-X-ray: Synchrotron radiation microbeam X-ray; JASRI: Japan Synchrotron Radiation Research Institute; XRF: X-ray fluorescence; XANES: X-ray absorption near edge structure; XRD: X-ray powder diffraction; SEM: Scanning electron microscope; RPV: Reactor pressure vessel

Acknowledgements

We thank all local governments for allowing us to investigate the SPM filter-tape samples. We are deeply grateful to Dr. Y Terada, Dr. K Nitta, and Dr. O Sekizawa (SPring-8/JASRI) for their assistances in the SR experiment at BL37XU, SPring-8. The synchrotron radiation experiments were performed with the approval of the SPring-8 Program Advisory Committee (proposal numbers 2016A1705, 2016B1811, 2017A1719, 2017B1757, 2018A1704, 2018B1748, and 2019B1308).

Authors' contributions

YA performed the SR measurements, data analysis, and wrote the manuscript. SO performed the separation of particles and SR measurements. IN and YI conceived the study idea. KA conducted the SEM analysis. YO and ME controlled the SPM filter-tape samples. TM and HN performed the trajectory analysis. KS conducted the gamma-ray spectrometry. HT and YM helped to devise the study idea and assisted with cooperation and coordination with local governments. All authors read and approved the final manuscript.

Funding

This work was supported by MEXT/JSPS KAKENHI Grants (24110003, 15H00978, 19H05702), in collaboration with projects of Environment Research and Technology Development Fund of the Environmental Restoration and Conservation Agency, Japan (JPMEERF20155001, JPMEERF20181002, and JPMEERF20192004). This work was also supported by Joint Research on Risk Evaluation and Management in Nuclear Technology (Japan-U.K.), the Collaborative Laboratories for Advanced Decommissioning Science, JAEA (JPJA18F18072860).

Availability of data and materials

Data sharing not applicable to this article as no datasets were generated or analyzed during the current study. Please contact corresponding author for data requests.

Competing interests

The authors declare that they have no known competing financial interests or personal relationships that could have appeared to influence the work reported in this paper.

Author details

[1]Department of Applied Chemistry, Faculty of Science, Tokyo University of Science, 1-3 Kagurazaka, Shinjuku-ku, Tokyo 162-8601, Japan. [2]Division of Material Science and Engineering, Graduate School of Engineering, Tokyo Denki University, 5 Senju Asahi-cho, Adachi-ku, Tokyo 120-8551, Japan. [3]Meteorological Research Institute, 1-1 Nagamine, Tsukuba-shi, Ibaraki 305-0052, Japan. [4]Institute for Integrated Radiation and Nuclear Science, Kyoto University, 2-chome, Asashiro-Nishi, Kumatori-cho, Sennan-gun, Osaka 590-0494, Japan. [5]College of Science, Ibaraki University, 2-1-1 Bunkyo, Mito-shi, Ibaraki 310-8215, Japan. [6]Graduate School of Science, Tokyo Metropolitan University, 1-1 Minami-Osawa, Hachioji-shi, Tokyo 192-0397, Japan. [7]Department of Earth Sciences, School of Education and Integrated Arts & Sciences, Waseda University, 1-6-1 Nishi-waseda, Shinjuku-ku, Tokyo 169-8050, Japan. [8]Research Center for Advanced Science and Technology, The University of Tokyo, 4-6-1 Komaba, Meguro-ku, Tokyo 153-8904, Japan.

[9]Japan Meteorological Business Support Center, 1-1 Nagamine, Tsukuba-shi, Ibaraki 305-0052, Japan. [10]Faculty of Pure and Applied Sciences, University of Tsukuba, 1-1-1 Tennodai, Tsukuba-shi, Ibaraki 305-8571, Japan. [11]Remote Sensing Technology Center of Japan, 3-17-1 Toranomon, Minato-ku, Tokyo 105-0001, Japan. [12]Department of Urban Engineering, The University of Tokyo, 7-3-1 Hongo, Bunkyo-ku, Tokyo 113-8656, Japan.

Received: 23 September 2020 Accepted: 21 December 2020
Published online: 26 January 2021

References

Abe Y, Iizawa Y, Terada Y, Adachi K, Igarashi Y, Nakai I (2014) Detection of uranium and chemical state analysis of individual radioactive microparticles emitted from the Fukushima nuclear accident using multiple synchrotron radiation X-ray analyses. Anal Chem 86:8521–8525. https://doi.org/10.1021/ac501998d

Adachi K, Kajino M, Zaizen Y, Igarashi Y (2013) Emission of spherical cesium-bearing particles from an early stage of the Fukushima nuclear accident. Sci Rep 3:2554. https://doi.org/10.1038/srep02554

Burns PT, Ewing RC, Navrotsky A (2012) Nuclear fuel in a reactor accident. Sci 225:1184–1188. https://doi.org/10.1126/science.1211285

Crouch EAC (1977) Fission-product yields from neutron-induced fission. At Data Nucl Data Tables 19:417–532. https://doi.org/10.1016/0092-640X(77)90023-7

Do TM, Sujatanond S, Ogawa T (2018) Behavior of cesium molybdate, Cs_2MoO_4, in severe accident conditions. (1) Partitioning of Cs and Mo among gaseous species. J Nucl Sci Technol 55:348–355. https://doi.org/10.1080/00223131.2017.1397560

Furuki G, Imoto J, Ochiai A, Yamasaki S, Nanba K, Ohnuki T, Grambow B, Ewing RC, Utsunomiya S (2017) Caesium-rich micro-particles: a window into the meltdown events at the Fukushima Daiichi Nuclear Power Plant. Sci Rep 7:42731. https://doi.org/10.1038/srep42731

Gouello M, Mutelle H, Cousin F, Sobanska S, Blanquet E (2013) Analysis of the iodine gas phase produced by interaction of CsI and MoO3 vapours in flowing steam. Nucl Eng Des 263:462–472. https://doi.org/10.1016/j.nucengdes.2013.06.016

Higaki S, Kurihara Y, Yoshida H, Takahashi Y, Shinohara N (2017) Discovery of non-spherical heterogeneous radiocesium-bearing particles not derived from Unit 1 of the Fukushima Dai-ichi Nuclear Power Plant, in residences five years after the accident. J Environ Radioact 177:65–70. https://doi.org/10.1016/j.jenvrad.2017.06.006

Igarashi Y, Kogure T, Kurihara Y, Miura H, Okumura T, Satou Y, Takahashi Y, Yamaguchi N (2019) A review of Cs-bearing microparticles in the environment emitted by the Fukushima Dai-ichi Nuclear Power Plant accident. J Environ Radioact 205–206:101–118. https://doi.org/10.1016/j.jenvrad.2019.04.011

Ikehara R, Morooka K, Suetake M, Komiya T, Kurihara E, Takehara M, Takami R, Kino C, Horie K, Takehara M, Yamasaki S, Ohnuki T, Law GTW, Bower G, Grambow B, Ewing RC, Utsunomiya S (2020) Abundance and distribution of radioactive cesium-rich microparticles released from the Fukushima Daiichi Nuclear Power Plant into the environment. Chemosphere 241:125019. https://doi.org/10.1016/j.chemosphere.2019.125019

Imoto J, Ochiai A, Furuki G, Suetake M, Ikehara R, Horie K, Takehara M, Yamasaki S, Nanba K, Ohnuki T, Law GTW, Grambow B, Ewing RC, Utsunomiya S (2017) Isotopic signature and nano-texture of cesium-rich micro-particles: release of uranium and fission products from the Fukushima Daiichi Nuclear Power Plant. Sci Rep 7:5409. https://doi.org/10.1038/s41598-017-05910-z

Itou K, Suzuki A, Ohishi Y, Nakamori F, Hikida S, Nozaki K, Honda T, Mizokami S (2018) Investigation of in-reactor cesium chemical behavior in TEPCO's Fukushima Daiichi Nuclear Power Station accident (10) Phenomenological generation mechanisms of spherical cesium bearing particle. In: Oral presentation in Atomic Energy Society of Japan 2018 Annual Meeting, held on 27 March 2018 at Osaka University Suita Campus

Kissane MP, Drosik I (2006) Interpretation of fission-product transport behaviour in the Phébus FPT0 and FPT1 tests. Nucl Eng Des 236:1210–1223. https://doi.org/10.1016/j.nucengdes.2005.10.012

Kurihara E, Takehara M, Suetake M, Ikehara R, Komiya T, Morooka K, Takami R, Yamasaki S, Ohnuki T, Horie K, Takehara M, Law GTW, Bower W, Mosselmans JFW, Warnicke P, Grambow B, Ewing RC, Utsunomiya S (2020a) Particulate plutonium released from the Fukushima Daiichi meltdowns. Sci Total Environ 743:140539. https://doi.org/10.1016/j.scitotenv.2020.140539

Kurihara Y, Takahata N, Yokoyama TD, Miura H, Kon Y, Takagi T, Higaki S, Yamaguchi N, Sano Y, Takahashi Y (2020b) Isotopic ratios of uranium and caesium in spherical radioactive caesium-bearing microparticles derived from the Fukushima Dai-ichi Nuclear Power Plant. Sci Rep 10:3281. https://doi.org/10.1038/s41598-020-59933-0

Martin PG, Jones CP, Cipiccia S, Batey DJ, Hallam KR, Satou Y, Griffiths I, Rau C, Richards DA, Sueki K, Ishii T, Scott TB (2020) Compositional and structural analysis of Fukushima-derived particulates using high-resolution X-ray imaging and synchrotron characterisation techniques. Sci Rep 10:1636. https://doi.org/10.1038/s41598-020-58545-y

Martin PG, Louvel M, Cipiccia S, Jones CP, Batey DJ, Hallam KR, Yang IAX, Satou Y, Rau C, Mosselmans JFW, Richards DA, Scott TB (2019) Provenance of uranium particulate contained within Fukushima Daiichi Nuclear Power Plant Unit 1 ejecta material. Nat Commun 10:2801. https://doi.org/10.1038/s41467-019-10937-z

MEXT (2020) Japanese Ministry of Education, Culture, Sports, Science and Technology. https://www.mext.go.jp/en/. Accessed 22 Nov 2020

Miura H, Kurihara Y, Sakaguchi A, Tanaka K, Yamaguchi N, Higaki S, Takahashi Y (2018) Discovery of radiocesium-bearing microparticles in river water and their influence on the solid-water distribution coefficient (K_d) of radiocesium in the Kuchibuto River in Fukushima. Geochem J 52:145–154. https://doi.org/10.2343/geochemj.2.0517

Miura H, Kurihara Y, Yamamoto M, Sakaguchi A, Yamaguchi N, Sekizawa O, Nitta K, Higaki S, Tsumune D, Itai T, Takahashi Y (2020) Characterization of two types of cesium-bearing microparticles emitted from the Fukushima accident via multiple synchrotron radiation analyses. Sci Rep 10:11421. https://doi.org/10.1038/s41598-020-68318-2

Nishihara K, Iwamoto H, Suyama K (2010) Estimation of fuel compositions in Fukushima-Daiichi nuclear power plant. In: JAEA-Data/Code 2012-018, Japan Atomic Energy Agency, 2010.

Okumura T, Yamaguchi N, Dohi T, Iijima K, Kogure T (2019) Dissolution behaviour of radiocaesium-bearing microparticles released from the Fukushima nuclear plant. Sci Rep 9:3520. https://doi.org/10.1038/s41598-019-40423-x

Ono T, Iizawa Y, Abe Y, Nakai I, Terada Y, Satou Y, Sueki K, Adachi K, Igarashi Y (2017) Investigation of the chemical characteristics of individual radioactive microparticles emitted from reactor 1 by the Fukushima Daiichi Nuclear Power Plant accident by using multiple synchrotron radiation X-ray analyses. Unseki Kagaku 66:251–261. https://doi.org/10.2116/bunsekikagaku.66.251

Onozaki S, Abe Y, Nakai I, Adachi K, Igarashi Y, Oura Y, Ebihara M, Miyasaka T, Nakamura H, Sueki K, Tsuruta H, Moriguchi Y (2019) Investigation of physical and chemical characteristics of radioactive aerosols emitted from reactor unit 1 by Fukushima Daiichi Nuclear Power Plant accident. BUNSEKI KAGAKU 68:757–768. https://doi.org/10.2116/bunsekikagaku.68.757

Oura Y, Ebihara M, Tsuruta H, Nakajima T, Ohara T, Ishimoto M, Katsumura Y (2015) Determination of atmospheric radiocesium on filter tapes used at automated SPM monitoring stations for estimation of transport pathways of radionuclides from Fukushima Dai-ichi Nuclear Power Plant. J Radioanal Nucl Chem 303:1555–1559. https://doi.org/10.1007/s10967-014-3662-4

Satou Y, Sueki K, Sasa K, Adachi K, Igarashi Y (2016) First successful isolation of radioactive particles from soil near the Fukushima Daiichi Nuclear Power Plant. Anthropocene 14:71–76. https://doi.org/10.1016/j.ancene.2016.05.001

Satou Y, Sueki K, Sasa K, Yoshikawa H, Nakama S, Minowa H, Abe Y, Nakai I, Ono T, Adachi K, Igarashi Y (2018) Analysis of two forms of radioactive particles emitted during the early stages of the Fukushima Dai-ichi Nuclear Power Station accident. Geochem J 52:145–154. https://doi.org/10.2343/geochemj.2.0514

Steinhauser G, Brandl A, Johnson TE (2014) Comparison of the Chernobyl and Fukushima nuclear accidents: a review of the environmental impacts. Sci Total Environ 470:800–817. https://doi.org/10.1016/j.scitotenv.2013.10.029

Suetake M, Nakano Y, Furuki G, Ikehara R, Komiya T, Kurihara E, Morooka K, Yamasaki S, Ohnuki T, Horie K, Takehara M, Law GTW, Bower W, Grambow B, Ewing RC, Utsunomiya S (2019) Dissolution of radioactive, cesium-rich microparticles released from the Fukushima Daiichi Nuclear Power Plant in simulated lung fluid, pure-water, and seawater. Chemosphere 233:633–644. https://doi.org/10.1016/j.chemosphere.2019.05.248

Takemura T, Nakamura H, Takigawa M, Kondo H, Satomura T, Miyasaka T, Nakajima T (2011) A numerical simulation of global transport of atmospheric particles emitted from the Fukushima Daiichi Nuclear Power Plant. SOLA 7:101–104. https://doi.org/10.2151/sola.2011-026

TEPCO (Tokyo Electric Power Co.) (2015) Examination into the reactor pressure increase after forced depressurization at Unit-2, using a thermal-hydraulic code. In: TEPCO reports latest findings of technical inquiry into how accident at Fukushima unfolded (2015) https://www.tepco.co.jp/en/press/corp-com/release/2015/1250927_6844.html. Accessed 22 Nov 2020

Terada Y, Goto S, Takimoto N, Takeshita K, Yamazaki H, Shimizu Y, Takahashi S, Ohashi H, Furukawa Y, Matsushita T, Ohata T, Ishizawa Y, Uruga T, Kitamura

H, Ishikawa T, Hayakawa S (2004) Construction and commissioning of BL37XU at SPring-8. AIP Conf Proc 705:376–379. https://doi.org/10.1063/1.1757812

Terada Y, Yumoto H, Takeuchi A, Suzuki Y, Yamauchi K, Uruga T (2010) New X-ray microprobe system for trace heavy element analysis using ultraprecise X-ray mirror optics of long working distance. Nucl Instrum Meth Phys Res A 616:270–272. https://doi.org/10.1016/j.nima.2009.12.030

Tsuruta H, Oura Y, Ebihara M, Moriguchi Y, Ohara T, Nakajima T (2018) Time-series analysis of atmospheric radiocesium at two SPM monitoring sites near the Fukushima Daiichi Nuclear Power Plant just after the Fukushima accident on March 11, 2011. Geochem J 52:103–121. https://doi.org/10.2343/geochemj.2.0520

Tsuruta H, Oura Y, Ebihara M, Ohara T, Nakajima T (2014) First retrieval of hourly atmospheric radionuclides just after the Fukushima accident by analyzing filter-tapes of operational air pollution monitoring stations. Sci Rep 4:6717. https://doi.org/10.1038/srep06717

Utsunomiya S, Furuki G, Ochiai A, Yamasaki S, Nanba K, Grambow B, Ewing RC (2019) Caesium fallout in Tokyo on 15th March, 2011 is dominated by highly radioactive, caesium-rich microparticles. https://arxiv.org/abs/1906.00212. Accessed 22 Nov 2020

Yamaguchi N, Mitome M, Akiyama-Hasegawa K, Asano M, Adachi K, Kogure T (2016) Internal structure of cesium-bearing radioactive microparticles released from Fukushima nuclear power plant. Sci Rep 6:20548. https://doi.org/10.1038/srep20548

Yamamoto T (2012) Radioactivity of fission product and heavy nuclides deposited on soil in Fukushima Dai-Ichi Nuclear Power Plant accident. J Nucl Sci Technol 49:1116–1133. https://doi.org/10.1080/00223131.2012.740355

Publisher's Note